Chemical Reactions between Aluminum and Fly Ash during Synthesis and Reheating of Al–Fly Ash Composite

R.Q. GUO and P.K ROHATGI

Thermodynamic analysis indicates that there is the possibility of chemical reactions between aluminum melt and cenosphere fly ash particles. These particles contain alumina, silica, and iron oxide, which, during solidification processing of aluminum–fly ash composites or during holding of such composites at temperatures above the melting temperature of aluminum, are likely to undergo chemical reduction. These chemical reactions between the fly ash and molten aluminum have been studied by metallographic examination, differential thermal analysis (DTA), scanning electron microscopy (SEM), energy-dispersive X-ray analysis (EDX) and X-ray analysis after holding the aluminum–fly ash composites for different periods above the liquidus temperature. The experiments indicate that there is progressive reduction of silica and mullite in the fly ash, and formation of alumina with holding time of composites at a temperature of 850 °C. The walls of the cenosphere fly ash particles progressively disintegrate into discrete particles as the reaction progresses. The rate of chemical reaction was high at the start of holding the composite at a temperature of 850 °C, and then the rate significantly decreased with time. The reaction was almost complete after 10 hours.

I. INTRODUCTION

SOLIDIFICATION processing has been used to make aluminum matrix composites, because this technique is the least expensive and best suited for fabrication of a variety of sizes and shapes of composite components.[1–7] During the last few years, fly ash, an industrial solid waste by-product, has been combined with molten aluminum to make low-cost aluminum matrix–fly ash particulate composites.[8,9,10] During processing, the molten aluminum or aluminum alloy is stirred with the fly ash before the composite is cast. Alternatively, loosely packed beds or preforms of fly ash can be infiltrated by molten aluminum under low or high pressure to form composites containing high volume fractions of fly ash. During solidification processing, there is an opportunity for chemical reaction between the aluminum and fly ash particles. The ashes are derived as oxides of the mineral content of the coals used, principally, in the thermal generation of electricity. The major components of fly ash are the oxides (and mixed metal oxides) of silicon, aluminum, iron, and calcium. Small amounts of the oxides of other common elements, such as magnesium and titanium, are also present. The phases present in fly ash particles were identified by X-ray diffraction.[11–15] These are quartz, mullite, lime, spinel, hematite, and ferrite. Some of the constituents may be partly amorphous.[14,16] Based on thermodynamic considerations, there is the possibility of chemical reactions between the aluminum melt and the constituents of fly ash such as SiO_2 and Fe_2O_3 or Fe_3O_4.[17,18,19] The elements reduced from fly ash (Si and Fe) would then alloy with the matrix aluminum. In sufficient quantity, these alloying elements can form intermetallic compounds with the aluminum and appear as second-phase precipitates in the castings. Such interfacial reactions between the metal matrix and the reinforcement fly ash particles would significantly influence the properties of the metal–fly ash interface, as well as the properties of the composites.[20,21,22]

In recent years, *in situ* synthesis has been reported for metal matrix–ceramic composites by reacting molten aluminum with amorphous silica,[23,24] aluminosilicate ceramic preforms,[25,26] and Al-Ti-C powder preforms,[27] or by reacting the molten Al-Ti alloy with CH_4.[28] The main constituents of the fly ash used in this study are SiO_2, Al_2O_3, and Fe_2O_3. The possible chemical reactions between molten aluminum and fly ash are shown as follows.[17,18,19]

$$2\ Al_{(l)} + 3/2\ SiO_{2(s)} = 3/2\ Si_{(s)} + Al_2O_{3(s)} \qquad (931 \text{ to } 1683 \text{ K}) \quad [1]$$

$$2\ Al_{(l)} + Fe_2O_{3(s)} = 2\ Fe_{(s)} + Al_2O_{3(s)} \qquad (950 \text{ to } 1033 \text{ K}) \quad [2]$$

At the experimental temperature of 850 °C, the Gibbs free energy changes in these chemical reactions are negative (−302,261 J/mole for Eq. [1] and −784,224 J/mole for Eq. [2]), indicating the possibility of chemical reactions between the molten aluminum and fly ash particles.

Progress of the chemical reactions between the aluminum and fly ash particles was studied using differential thermal analysis (DTA). The microstructure of the resulting samples was observed through optical microscopy and scanning electron microscopy (SEM). The change in the chemical composition of both the fly ash particles and the aluminum matrix due to the chemical reactions was examined by energy-dispersive X-ray (EDX) analysis. The constituents of the fly ash, as well as the aluminum matrix, were confirmed by X-ray diffraction before and after the chemical reaction.

II. EXPERIMENTAL PROCEDURE

A. *Sample Preparation*

Commercially pure aluminum pellets (99.9 pct Al) and cenosphere fly ash (hollow particles) collected from a Ci-

R.Q. GUO, Postdoctoral Fellow, and P.K. ROHATGI, Professor, are with the Department of Materials, University of Wisconsin–Milwaukee, Milwaukee, WI 53201.

Manuscript submitted June 13, 1997.

Table I. Chemical Composition of Pure Aluminum (Parts per Million)

Fe	Ga	V	Zn	Ni	Cu	Mg	Ca	Zr	Al
320	55	20	15	9	8	3	1	1	bal

nergy Corporation (Cincinnati, OH) power plant were used in this experimental work. The chemical compositions of the pure aluminum and fly ash are given in Tables I and II, respectively. The fly ash contains 61 wt pct SiO_2, 26 wt pct Al_2O_3, and less than 5 wt pct iron oxide. The X-ray diffraction pattern of this fly ash (Figure 1) shows that the phases present are largely silica (SiO_2), alumina (Al_2O_3), and mullite ($3Al_2O_3 \cdot 2SiO_2$).

Pure aluminum–cenosphere fly ash composite samples were prepared by a low-pressure infiltration technique. This technique involves pressurizing molten aluminum over a bed of loose fly ash powder to produce composites containing about 40 vol pct of the hollow cenosphere fly ash. A graphite mold containing the fly ash was heated to near the melting point of aluminum. Then, the liquid metal, at 700 °C, was poured into the mold and squeezed vertically, by a graphite ram attached to a hydraulic compressor, to a gage pressure of 0.7 MPa.

The aluminum–cenosphere fly ash composite bar was then sectioned into two half-cylinders. One of them was loaded with a similarly sized pure aluminum half-cylinder piece (99.9 pct Al, remelted and cast in a mold from commercially pure aluminum pellets) into a graphite crucible used for vacuum remelting and holding experiments. The graphite crucible was held in a vacuum furnace at 1.33×10^{-3} Pa and heated at the rate of 50 °C/min to 850 °C, then held for times of 0.5 to 27 hours to obtain different chemical reaction products before being cooled in the furnace under vacuum. The resulting sample is half composite–half aluminum without fly ash particles, as shown in Figure 2. The study of the reactions in contact with the half-cylinder of pure aluminum was done to accelerate the reactions between the aluminum and fly ash. The reaction products like silicon and iron, formed as a result of the reduction of their oxides in fly ash by molten aluminum, will accumulate in the liquid aluminum when chemical reaction occurs between molten aluminum and fly ash. This will result in an increase in the concentrations of silicon and iron in the small volumes of molten aluminum between the fly ash particles, since both silicon and iron are soluble in the melt. This raises the activity of these elements in the melt, thereby slowing down the forward reaction. By placing a half-cylinder of commercially pure aluminum in contact with the composite samples, and melting it, the silicon and iron reduced from fly ash were able to diffuse to the pure aluminum side, thereby reducing their build up in the molten matrix in the composite side. This will prevent the slowing down of the reduction reaction due to a build up of silicon and iron in the matrix. The half-cylinder of pure aluminum provided a sink for the reaction products like silicon and iron, resulting from the reactions between the aluminum and the fly ash, on the composite side of the sample. Therefore, the half-cylinder of pure aluminum in contact with the composite will result in faster reactions between the aluminum and fly ash, as compared to the case when no pure aluminum cylinder is present.

B. *Characterization of Sample*

An optical microscope (Olympus/BH2-UMA) was used to study the microstructure of aluminum–fly ash composites. The volume percentage of cenosphere fly ash particles in the aluminum–cenosphere fly ash composite was measured on polished samples by a LECO* 2001 image analyzer. Standard polishing procedures were followed using SiC grinding papers to 600 grit. Final polishing was done on a micropolishing cloth with a 0.05 μm SiO_2 slurry.

*LECO is a trademark LECO Corporation, St. Joseph, MI.

The DTA apparatus used in this research was a DuPont model 2000. Analyses were carried out with nitrogen (flow rate: less than 1 cm^3/s) as the furnace atmosphere. Alumina crucibles were used for sample holders and α-alumina powder was used as the reference material. The heating and cooling rates were 10 °C/min. Areas under the peaks on the DTA curve were integrated to calculate the heat released by phase transitions or chemical reactions. This heat, ΔH, can be calculated by the equation[29]

$$\Delta H = K S \qquad [3]$$

where K is a constant and S is the peak area of the DTA curve. The constant value K can be calculated using handbook data for ΔH and DTA measurements for S.

Scanning electron microscopy was used to investigate the details of the cenosphere fly ash disintegration due to the chemical reactions between aluminum and fly ash. The SEM used in this study was a Topcon ABT-32 system.

The samples were studied by means of X-ray diffraction, carried out in a Scintag XDS 2000 unit. The structure of the aluminum matrix, the phase components of the fly ash particles, and the phase change in the fly ash particles during the synthesis of composite due to the chemical reaction were determined. The structure of precipitates in the aluminum matrix, formed during solidification, was also confirmed by X-ray analysis.

III. RESULTS AND DISCUSSION

A. *Microscopic Examination*

Figure 3 shows the micrographs of an aluminum–cenosphere fly ash composite without soaking and a ''half-and-half'' sample soaked at 850 °C for 5 hours. In Figure 3(a), of the pressure-infiltrated sample prior to any soaking, the aluminum matrix appears as single phase and the cenosphere particles have a smooth surface. Figure 3(b) shows the microstructure of the half-and-half sample after soaking at 850 °C for 5 hours. The presence of second-phase particles in the matrix, which was originally pure aluminum, can be seen. The cenosphere particles do not migrate from the composite side to the pure aluminum side of the cylinder during the process, as seen in Figure 3(b). The silicon and iron did diffuse into the pure aluminum half of the sample and reacted to form the second-phase particles during solidification. The figure also shows that the cenospheres appear to be cracked, with fine particles along the periphery of the original wall of the particles, presumably due to chemical reactions. According to the thermodynamic analyses, it is likely that silica or one or both of the iron

Table II. Weight Percentage of Different Chemical Constituents of Cenosphere Fly Ash

Oxide	SiO_2	Al_2O_3	Fe_2O_3	CaO	MgO	MnO	NaO	P_2O_5	TiO_2	SO_3	LOI*
Wt pct	61.02	25.79	4.99	0.82	1.58	0.02	0.74	0.09	1.00	0.31	3.64

*LOI: loss of ignition.

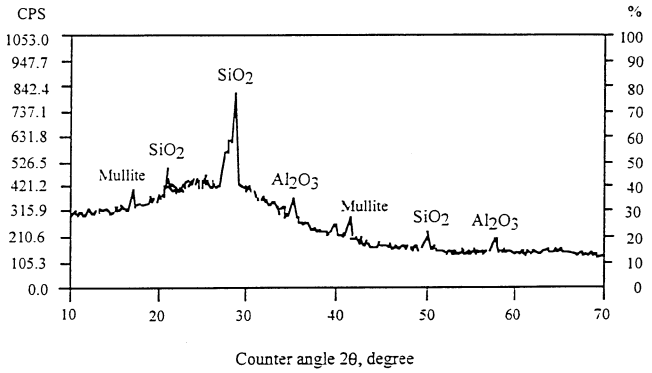

Fig. 1—X-ray diffractogram of cenosphere fly ash used in this research.

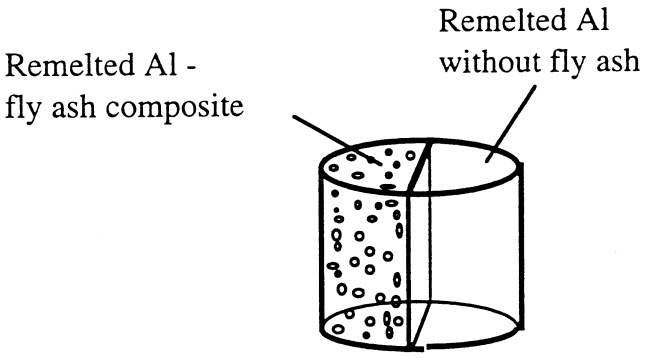

Fig. 2—A sketch of the resulting sample with half composite and half aluminum.

oxides were reduced by molten aluminum. The aluminum-silicon phase diagram shows that the solidification of a hypoeutectic alloy can be described as follows.

The eutectic composition is approximately 12 wt pct Si. Below this concentration, aluminum solidifies with α—aluminum—silicon solid solution as the primary phase in the form of dendrites. Even if all of the original silica present in the fly ash (60 wt pct SiO_2) were reduced to the element Si in the composite-half part (40 vol pct or 12 wt pct fly ash) of the sample, the silicon content in the aluminum in the composite part would be approximately 3.5 wt pct. When the temperature of the cooling sample reached the eutectic temperature, the remaining liquid would transform into interdendritic α plus essentially pure silicon. Before the chemical reactions between cenosphere fly ash and molten aluminum, the cenosphere fly ash particles were near spherical with very clean and smooth surfaces, as shown in Figure 3(a). It can be seen from this figure that the majority of the particles are unbroken and possess an uncracked surface. Even though the cenosphere fly ash was in contact with molten aluminum during pressure infiltration for a short period of time (less than 10 minutes), the cenosphere fly ash particles still retained a relatively clean surface and a close-to-spherical shape, as shown in Figure 3(a). This was because, at most, only a very small quantity of oxides

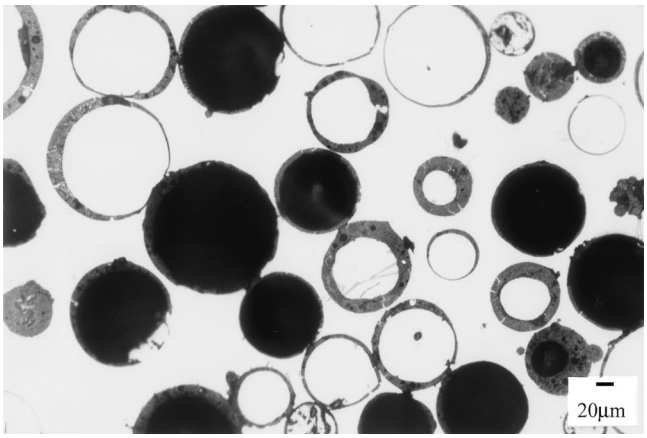

(*a*)

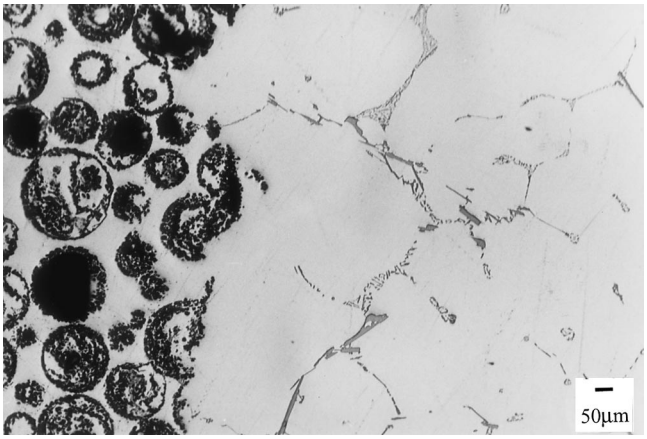

(*b*)

Fig. 3—Photomicrographs of aluminum–cenosphere fly ash composite produced by pressure infiltration: (*a*) prior to soaking and (*b*) half-and-half sample soaked at 850 °C for 5 h.

in the cenosphere wall had been reduced by molten aluminum during that short contact time.

With longer soak times at 850 °C, increasing amounts of chemical reaction occurred between the molten aluminum and the cenosphere fly ash particles. Larger amounts of silicon and iron compounds were reduced. The resulting alloying elements formed second phases and precipitated during the solidification of both sides of the samples, although it is easier to observe these phases in the aluminum side of the sample. The resulting structure of the cenosphere fly ash is shown in Figure 3(b). It does not have a smooth hollow particle shape, but a ''spherical wall'' that has formed from the residual disintegrated and unreacted wall material, along with coarse precipitates formed as a result of the reaction between the molten aluminum and fly ash. However, the overall spherical shape of the original wall is still maintained.

The chemical reduction reaction between molten alumi-

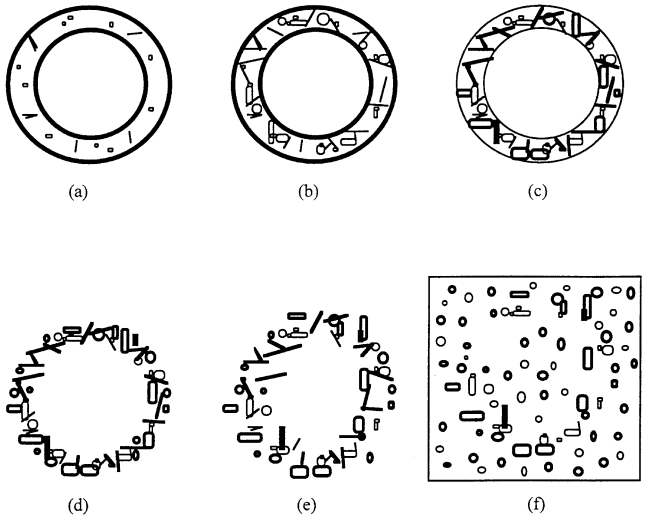

Fig. 4—Schematic views showing change in cenosphere fly ash due to chemical reaction between fly ash particles and aluminum: (*a*) original cenosphere fly ash particle with small cracks and pores in the wall of the cenosphere; (*b*) more cracks and pores due to some SiO_2 and Fe_2O_3 reduced by molten aluminum forming Al_2O_3; (*c*) more cracks and cenosphere wall being broken into small pieces due to further SiO_2 and Fe_2O_3 reduction; (*d*) remaining unreacted particles of cenosphere fly ash as well as newly formed Al_2O_3 particles; (*e*) small particles moved slightly from the original positions near the wall of cenosphere, but the original cenosphere wall shape still observable; (*f*) small particles formed by chemical reactions moving away from their original position near the cenosphere wall and becoming uniformly distributed in the matrix after still longer times.

num and fly ash appears to occur in several steps, as follows.

(1) The initial chemical reaction and wall fracture occur.
(2) The metallic elements (Si and Fe), formed as a result of the reaction between aluminum and fly ash, migrate away from the interface by diffusion and convection.
(3) The remaining unreacted oxides of the fly ash cenosphere wall and the newly formed aluminum oxide continue to occupy positions close to their original positions in the wall.
(4) With longer soaking times, the particles remaining from the original fly ash and those newly formed as a result of reaction migrate away from their original positions near the cenosphere wall and become uniformly distributed in the matrix.

Steps 2 and 3 describe the transport of the reaction products through the melt, as well as near the wall, of the cenosphere fly ash. The rate of these transport processes will be determined by the chemical driving forces dictated by temperature and fly ash chemistry, and by the appropriate transport coefficients. The latter will depend upon any defects in the wall such as cracks or pores and, in certain cases, upon the microstructure of the reaction product, since, for instance, liquid could enter through cracks or pores in the wall and initiate reaction from inside at an early stage.

Figure 4 schematically shows the change in the morphology of the cenosphere fly ash due to the chemical reactions between aluminum and fly ash. There are few cracks and pores in the wall of the original cenosphere particles. As chemical reaction between the fly ash particles and molten aluminum progressed, increasing numbers of cracks and pores of larger sizes appeared. This is apparently due to increasing amounts of silicon and iron oxides in the cenosphere wall being progressively reduced by molten aluminum, as shown in Figures 4(b) and (c). The metallic elements such as silicon and iron, formed as a result of the reaction between silicon and iron oxides in the fly ash and molten aluminum, dissolved into the molten aluminum. After still longer soaking times, remaining portions of unreacted fly ash particles, as well as the alumina reaction product deposited on them, moved only slightly from their original positions near the wall of the cenosphere, and the cenosphere wall shape still could be observed (Figures 4(d) and (e)). After longer soaking times, the residual fly ash particles and the newly formed particles resulting from the reaction move away from their original positions near the cenosphere wall and become uniformly distributed in the matrix, as shown in Figure 4(f).

Figure 5 shows the SEM micrographs of cenosphere fly ash, as well as an aluminum–cenosphere fly ash composite produced by low-pressure infiltration and soaked in a vacuum furnace at 850 °C for different lengths of time. These SEM pictures show that the cenosphere fly ash particle disintegrates due to the chemical reaction with molten aluminum. The original cenosphere exhibits a spherical shape and smooth surface, as shown in Figure 5(a). There is not much change in cenosphere particle wall after soaking for 0.5 hours, as shown in Figure 5(b). As cenosphere fly ash particles remain in contact with molten aluminum for longer times, greater amounts of silicon and iron oxides in the cenosphere wall are reduced by molten aluminum, and the cenosphere wall appears broken, as shown in Figure 5(c). The reduced metallic elements, largely silicon and iron, dissolved into molten aluminum, and some migrated to the pure aluminum side of the sample to precipitate as silicon- and iron-rich phases. As shown in Figure 5(d), after soaking for 27 hours, the fine particles, the unreacted parts of the cenospheres, and the chemical reaction products became more uniformly distributed in the aluminum matrix.

B. *DTA and X-ray Diffraction*

The results of DTA during solidification are illustrated in Figure 6 for the pure aluminum and aluminum half-cylinder after contact with the aluminum–cenosphere fly ash composites for 1 hour at 850 °C. A major solidification exotherm occurred at a nucleation temperature of 655 °C for the pure aluminum (curve (a) in Figure 6). Since chemical reactions between the molten aluminum and fly ash particles took place during the processing, some of the silicon and iron oxides were reduced by the molten aluminum and the silicon, and iron diffused into the fly ash–free half-cylinder (as shown in Figure 3(b)). In comparison to the DTA curve of pure aluminum, the DTA curve of the fly ash–free portion of the sample, which originally was pure aluminum, shows a second peak on the curve, shown in Figure 6 as curve (b). This lower temperature peak (565 °C) is most likely due to eutectic reaction. A slightly lower aluminum nucleation temperature of 652 °C is noted for this material, because it contains some dissolved elements (silicon and iron), which were reduced from the fly ash cenospheres.

The phases present in the fly ash used in this research were determined by X-ray diffraction analysis, as shown in

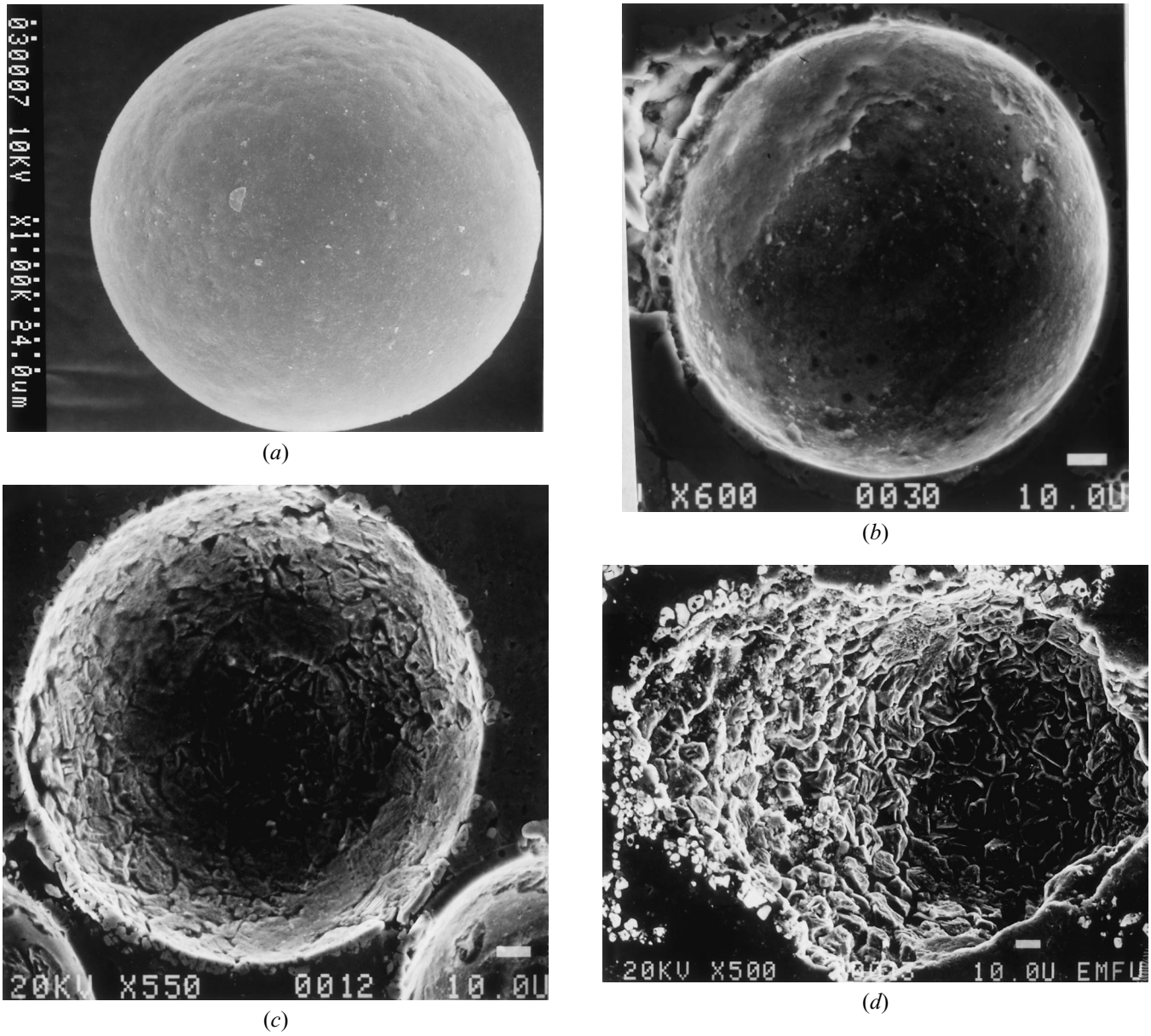

(*a*) (*b*) (*c*) (*d*)

Fig. 5—SEM micrographs of cenosphere fly ash as well as pure aluminum–cenosphere fly ash composite produced by pressure infiltration and soaked in a vacuum furnace at 850 °C for different times, showing cenosphere particle disintegrating due to the chemical reaction between molten aluminum and cenosphere fly ash: (*a*) original cenosphere, (*b*) soaked for 0.5 h, (*c*) soaked for 5 h, and (*d*) soaked for 27 h.

Figure 1. The majority of the crystalline components of this cenosphere fly ash are silica (SiO_2), alumina (Al_2O_3), and mullite ($3Al_2O_3{\cdot}2SiO_2$). After chemical reaction between the cenosphere particles and the molten aluminum, the phases present in the cenosphere fly ash changed. Figure 7 shows the X-ray diffractogram of an aluminum–cenosphere fly ash composite produced by the low-pressure infiltration technique and soaked at 850 °C for 0.5 hours. It can be seen that there are relatively smaller peaks of $3Al_2O_3{\cdot}2SiO_2$ (mullite) on the X-ray diffractogram, even after soaking for a short time. As soaking time is extended, there are no peaks of $3Al_2O_3{\cdot}2SiO_2$ (mullite) or SiO_2 on the X-ray diffractogram, as shown in Figure 8, indicating that all of the mullite present in the fly ash has been reduced after 5 hours of reaction time. Relatively strong peaks of silicon were present for the samples with longer soaking times, presumably due to the formation of metallic elements as a result of the reduction of silicates in the fly ash and the subsequent diffusion of these elements. The disintegration of cenosphere fly ash particles has been observed as a function of soaking time, as the chemical reaction occurred between them and molten aluminum (Figure 5). As the chemical reaction progressed, increasing amounts of silicon and iron were reduced from the cenosphere walls by molten aluminum surrounding the fly ash particle. The resulting structure of the cenosphere fly ash appeared to contain progressively greater amounts of Al_2O_3.

Figure 9 gives the variations of the X-ray intensity (I), ratios of silicon to aluminum, and silica reduction rate, determined by DTA as a function of soaking time. It is noted from the DTA curve that the reaction, at the beginning, between aluminum and fly ash was very fast. As soaking time increased, the average reaction rate significantly decreased, and only a small amount of silicon would be re-

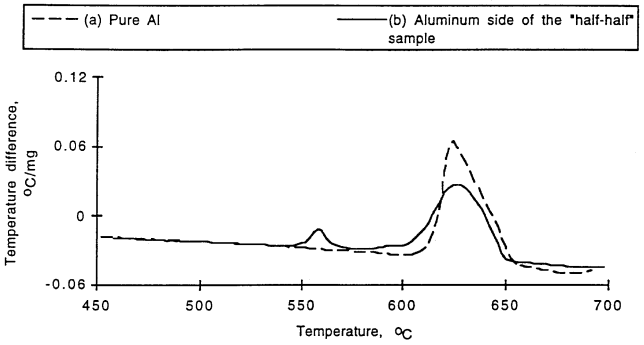

Fig. 6—DTA curves: cooling rate—10 °C/min; furnace atmosphere—N_2; and reference material—alumina: (*a*) pure aluminum and (*b*) aluminum side of the aluminum–cenosphere fly ash composite (the part of the sample that did not contain fly ash, soaked at 850 °C, 1 h).

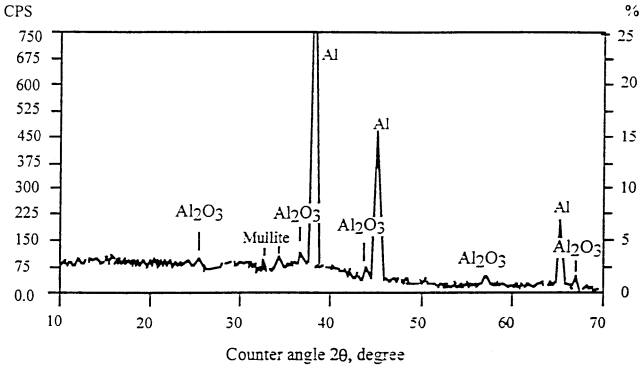

Fig. 7—X-ray diffractogram of aluminum–cenosphere fly ash composite produced by pressure infiltration technique; soaked at 850 °C for 0.5 h.

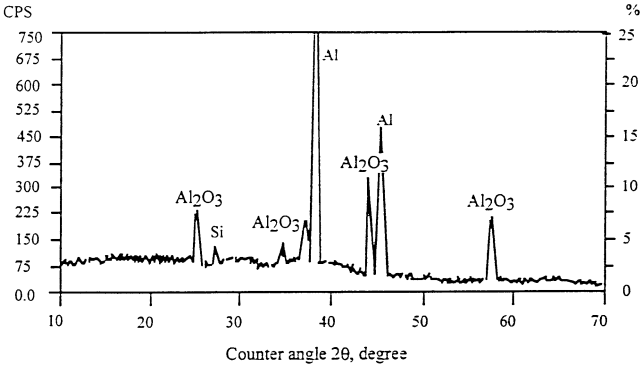

Fig. 8—X-ray diffractogram of aluminum–cenosphere fly ash composite produced by pressure infiltration, soaked at 850 °C for 5 h.

leased during the DTA test. This decrease is due to a film of the reaction product, Al_2O_3, deposited on the remaining fly ash particles and to the fact that much of the silica has already reacted with aluminum and, thus, the contact area between the molten aluminum and silica has decreased. Previous investigations show that the solid-film thickness greatly affects the rate of subsequent Al-SiO_2 reactions.[30] The total silicon reduced from fly ash can be calculated by integrating the DTA curve from 0 to 10 hours. The silicon content in the aluminum matrix of the composite side will be approximate to 4 to 4.6 wt pct, very close to the 3.5 wt pct calculated. It can be seen from the figure that the relative X-ray intensity of I_{Si}/I_{Al} increased, as soaking time

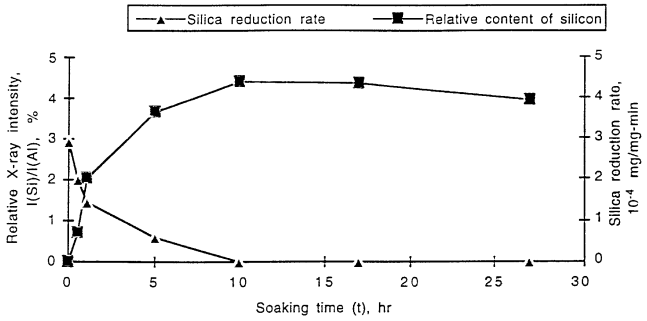

Fig. 9—The variation of average chemical reaction rate between aluminum and fly ash with soaking time at the temperature range of 650 C° to 700 °C determined by DTA and the relative intensity of X-ray diffraction for samples taken from pure aluminum portion in half-and-half cylinder.

Table III. The Results of EDX Examination on Cenosphere Fly Ash Particle

Sample condition	Al_2O_3	SiO_2	Fe_2O_3
Original cenosphere	36.8 to 41.1	45.0 to 52.0	1.65 to 2.89
Cenosphere in composite (850 °C, 0.5 h)	77.4	15.2	6.42
Cenosphere in composite (850 °C, 5 h)	94.5 to 99.8	0.11 to 5.02	0 to 0.22

increased to 10 hours, for the samples taken from the part of the cylinder that was initially pure aluminum. After soaking for 10 hours, I_{Si}/I_{Al} is almost constant. This means that the silicon content in the composite reached its maximum value and there was little further reaction between the aluminum and fly ash particles.

C. *EDX Examination*

For the sample shown in Figure 5(c), there are many small particles occupying sites near the original wall position of the cenosphere. It is believed that these particles are the remaining unreacted parts of the cenosphere and the new particles formed as a result of the chemical reaction. Their chemical composition was examined by EDX. The results of the EDX quantity analysis are given in Table III.

Since chemical reactions took place whenever the molten aluminum contacted the fly ash particles, different amounts of reactants such as SiO_2 and Fe_2O_3, or Fe_3O_4, were reduced after different soak times at 850 °C. As the chemical reactions progress, increasing amounts of Al_2O_3 were seen in the resulting structure of cenosphere fly ash. Meanwhile, the particles contained progressively smaller amounts of SiO_2. The remaining particles in the cenosphere fly ash wall contained as much as 94.5 to 99.8 wt pct of Al_2O_3 for the sample soaked at 850 °C for 5 hours, compared to 77.4 wt pct and 36.8 to 41.1 wt pct of Al_2O_3 for the samples soaked at 850 °C for 0.5 hours and those in their original state, respectively.

Table IV gives the results of EDX quantity analysis for the aluminum part of the half-and-half sample. The chemical composition of the α-aluminum crystal shows reasonably low impurity elements, as expected. There is a significant variation of concentrations for the interdendritic regions. This is because the EDX measuring point covered different locations in the Al-Si eutectic structure. The chemical composition of the second phase in the aluminum

Table IV. The Results of EDX Examination on the Aluminum Side of the Half-and-Half Sample

Examination Position	Al	Si	Fe	Ca	Mn	K	Other
α-Aluminum crystal	98.8 to 98.9	0.14 to 0.24	0.26 to 0.29	0.08 to 0.11	0 to 0.17	0	0.43 to 0.60
Interdendritic regions	26.6 to 91.3	7.02 to 71.7	0 to 1.15	0 to 0.22	0 to 0.41	0 to 0.08	0.29 to 1.16
Second phase in Al	62.5	10.7	26.7	0	0	0.10	0

matrix exhibits almost same value as that of the Al_5FeSi phase (61.6 wt pct Al, 25.6 wt pct Fe, and 12.8 wt pct Si). The reaction during solidification, liquid $\rightarrow$ α-Al + Si + Al_5FeSi, has already been proven for an AlSi alloy.[31]

IV. CONCLUSIONS

1. Chemical reactions between aluminum and cenosphere fly ash particles occur at temperatures of 700 °C to 850 °C.
2. Elements such as silicon and iron are effectively reduced by molten aluminum from their oxides in the fly ash particles during synthesis and reheating of the aluminum–fly ash composite.
3. The solidification temperature of the aluminum melt decreased, compared to pure aluminum, due to an enrichment in Si and Fe resulting from the reduction of Si and Fe from the SiO_2 and Fe_2O_3 of the cenosphere into the melt.
4. The remaining particles contained a very high percentage of Al_2O_3 and occupied their original positions in the cenosphere wall for certain soak times.
5. The structure of the aluminum matrix is the same as in a common aluminum-silicon alloy, exhibiting α-aluminum dendrites with an aluminum-silicon eutectic and an AlSiFe-precipitated phase in it.
6. An X-ray diffractogram of the as-received cenosphere fly ash shows that there is Al_2O_3, SiO_2, and mullite,as well as a great amount of amorphous phase, in the fly ash. As a result of the chemical reaction between molten aluminum and the cenosphere fly ash, the SiO_2 and mullite phases in the fly ash appear to have been progressively consumed, and increasing amounts of Al_2O_3 compound formed after about 5 hours of reaction at 850 °C. There is, then, no detectable SiO_2 and mullite left in the fly ash.

REFERENCES

1. D.J. Lloyd: *Int. Mater. Rev.*, 1994, vol. 39, pp. 1-23.
2. J.T. Burke, C.-C. Yang, and S.J. Canino: *Trans. Am. Foundrymen's Soc.*, 1994, vol. 102, pp. 585-91.
3. S. Ray: *J. Met. Sci.*, 1993, vol. 28, pp. 5397-5413.
4. K.K. Chawla: *Composite Materials*, Springer-Verlag, New York, NY, 1987, pp. 177-78.
5. X.S. Ning, T. Okamoto, Y. Miyamoto, and A. Koreeda: *J. Met. Sci.*, 1991, vol. 26, pp. 2050-56.
6. P. Rohatgi and R. Asthana: *JOM*, 1991, May, pp. 35-41.
7. D.O. Kennedy and J.C. Church: *Trans. Am. Foundrymen's Soc.*, 1991, vol. 99, pp. 142-48.
8. P.K. Rohatgi: *JOM*, 1994, Nov., pp. 55-58.
9. D. Golden: *EPRI J.*, 1994, Jan.–Feb., pp. 46-49.
10. P.K. Rohatgi, R. Guo, B.N. Keshavaram, and D.M. Golden: *Trans. Am. Foundrymen's Soc.*, 1995, vol. 103, pp. 575-79.
11. R.T. Hemmings and E.E. Berry: *Mater. Res. Soc. Symp. Proc.*, 1985, vol. 65, pp. 91-104.
12. N. Kaufherr, M. Shenasa, and D. Lichtman: *Environ. Sci. Technol.*, 1985, vol. 19, pp. 609-14.
13. D. Lichtman and S. Mroczkowski: *Environ. Sci. Technol.*, 1985, vol. 19, pp. 274-77.
14. D.M. Roy, K. Luke, and S. Diamond: *Mater. Res. Soc. Symp. Proc.*, 1985, vol. 43, pp. 3-20.
15. G.M. Idorn: *Mater. Res. Soc. Symp. Proc.*, 1985, vol. 65, pp. 3-10.
16. R.B. Finkelman: *Mater. Res. Soc. Symp. Proc.*, 1985, vol. 65, pp. 71-76.
17. R.C. Weast: *CRC Handbook of Chemistry and Physics*, 70th ed., CRC Press, Inc., Boca Raton, FL, 1990, p. D-33.
18. G.V. Samsonov: *The Oxide Handbook*, IFI/Plenum Data Corporation, New York, NY, 1973, pp. 122-24.
19. S.J. Schneider: *Engineering Materials Handbook*, ASM INTERNATIONAL, Materials Park, OH, 1991, vol. 4, pp. 747-48.
20. P.M. Scott, M. Nicholas, and B. Dewar: *J. Met. Sci.*, 1975, vol. 10, pp. 1833-40.
21. J.H. Perepezko: *Composite Interfaces*, 1993, vol. 1, pp. 463-80.
22. J.M. Howe: *Int. Mater. Rev.*, 1993, vol. 38, pp. 257-71.
23. M.C. Breslin, J. Ringnalda, J. Seeger, A.L. Marasco, G.S. Daehn, and H.L. Fraser: *Ceram. Eng. Sci. Proc.*, 1994, vol. 15 (4), pp. 104-12.
24. S. Matsuo and T. Inabe: *Tokyo Ceram.*, 1991, pp. 222-23.
25. R.E. Loehman, K.G. Ewsuk, and A.P. Tomsia: *J. Am. Ceram. Soc.*, 1996, vol. 79 (1), pp. 27-32.
26. K.G. Ewsuk, S.J. Glass, R.E. Loehman, A.P. Tomsia, and W.G. Fahrenholtz: *Metall. Mater. Trans. A*, 1996, vol. 27A, pp. 2122-29.
27. T. Nukami and M.C. Flemings: *Metall. Mater. Trans. A*, 1995, vol. 26A, pp. 1877-84.
28. P. Sahoo and M.J. Koczac: *Mater. Sci. Eng.*, 1991, vol. A131, pp. 69-73.
29. W.J. Smothers and Y. Chiang: *Handbook of Differential Thermal Analysis*, Chemical Publishing Company, Inc., New York, NY, 1966, pp. 124-55.
30. K. Prabriputaloong and M.R. Piggott: *J. Am. Ceram. Soc.*, 1973, vol. 56 (4), pp. 177-80.
31. L. Bäckerud, G. Chai, and J. Tamminen: *Solidification Characteristics of Aluminum Alloys*, AFS/Skanaluminum, Stockholm, Sweden, 1986, vol. 2, pp. 8-10.